Magnetic Resonance Imaging 61 (2019) 158–166

Contents lists available at ScienceDirect

Magnetic Resonance Imaging

journal homepage: www.elsevier.com/locate/mri

Original contribution

Improved synthetic T1-weighted images for cerebral tissue segmentation in neurological diseases

René-Maxime Gracien[a,c,f,*], Alexandra van Wijnen[a,b,c], Michelle Maiworm[a,b,c,f], Franca Petrov[a,c], Nina Merkel[a,c,e,f], Esther Paule[a,c,f], Helmuth Steinmetz[a,f], Susanne Knake[d,f], Felix Rosenow[a,f], Marlies Wagner[b,c,f], Ralf Deichmann[c,f]

[a] Department of Neurology, Goethe University, Frankfurt/Main, Germany
[b] Department of Neuroradiology, Goethe University, Frankfurt/Main, Germany
[c] Brain Imaging Center, Goethe University, Frankfurt/Main, Germany
[d] Department of Neurology, Phillips University, Marburg, Germany
[e] Ernst Strüngmann Institut for Neuroscience in cooperation with Max Planck Society, Frankfurt/Main, Germany
[f] Center for Personalized Translational Epilepsy Research (CePTER) Consortium, Germany

ARTICLE INFO

Keywords:
Synthetic images
Quantitative MRI
T1
PD
Epilepsy
Focal cortical dysplasia
Multiple sclerosis (MS)

ABSTRACT

Structural cerebral MRI analysis in patients with neurological diseases usually requires T1-weighted datasets for tissue segmentation. For this purpose, synthetic T1-weighted images which are constructed from quantitative maps of the underlying tissue parameters such as the T1 relaxation time and the proton density (PD) may provide advantages over conventional datasets. However, in some cases synthetic images may suffer from specific artifacts, hampering accurate tissue segmentation.

The goal was to improve a previously described method for the calculation of synthetic magnetization-prepared rapid gradient-echo (MP-RAGE) datasets from quantitative T1 and PD maps. Improvements comprise a B0-correction for the water-selective excitation pulses employed in T1-mapping and the use of T1-based pseudo-PD maps.

Synthetic T1-weighted MP-RAGE datasets were calculated, using the standard and the improved algorithm, for 10 patients with focal epilepsy (caused by focal cortical dysplasia in 9), 10 patients with multiple sclerosis and 10 healthy control subjects and segmented with the Freesurfer toolbox.

Visual inspection disclosed that segmentation of the standard synthetic datasets was inaccurate in 6 out of 10 patients with epilepsy, 7 out of 10 patients with multiple sclerosis and 7 out of 10 healthy control subjects, while the improved synthetic datasets resulted in adequate segmentation outcomes in the majority of cases. Only for one patient with multiple sclerosis and one with epilepsy, segmentation in basal temporal regions was not sufficient.

Furthermore, data based on the standard algorithm showed strong signal non-uniformities in basal regions. This effect was not present in the improved synthetic datasets.

1. Introduction

Quantitative MRI (qMRI) analyses allow for the quantification of tissue parameters and thus may aid the assessment of diffuse tissue pathologies which might remain undetected in conventional clinical MRI data [1]. As an example, the application of qMRI techniques in multiple sclerosis (MS), a chronic inflammatory disease of the central nervous system (CNS), allows to gain insights into pathological changes of normal appearing tissues outside of the obvious lesions [2]. Previous studies have shown that these changes are related to the clinical status of the respective patients [3–5]. In the field of epilepsy, where conventional MRI data frequently fail to show any pathological structural

Abbreviations: BW, bandwidth; CNS, central nervous system; DTI, diffusion tensor imaging; FOV, field-of-view; FSL, FMRIB Software Library; GE, gradient echo; GLM, general linear model; GM, gray matter; MP-RAGE, magnetization-prepared rapid gradient-echo; MS, multiple sclerosis; PD, proton density; qMRI, quantitative MRI; RF, radio frequency; RP, receive coil profile; RRMS, relapsing-remitting MS; SNR, signal-to-noise ratio; SPM, Statistical Parametric Mapping; T, tesla; VFA, variable flip angle; WM, white matter

* Corresponding author at: Brain Imaging Center, University Hospital, Schleusenweg 2-16, 60528 Frankfurt, Germany.
E-mail address: Rene-Maxime.Gracien@kgu.de (R.-M. Gracien).

https://doi.org/10.1016/j.mri.2019.05.013
Received 20 February 2019; Received in revised form 11 April 2019; Accepted 6 May 2019
0730-725X/ © 2019 Elsevier Inc. All rights reserved.

changes [6], qMRI data may help to distinguish between patients and healthy subjects [7,8].

However, the analysis of qMRI data requires reliable tissue segmentation. For this purpose, T1-weighted anatomical datasets are commonly acquired and segmented with toolboxes such as the FMRIB Software Library (FSL, FMRIB, Oxford), FreeSurfer (Athinoula A. Martinos Center for Biomedical Imaging, Boston) or "Statistical Parametric Mapping" (SPM, Wellcome Department of Imaging Neuroscience, UCL, London). T1-weighted Magnetization-Prepared Rapid Acquisition of Gradient Echoes (MP-RAGE) datasets are particularly well suited for tissue segmentation with these toolboxes.

In general, conventional MP-RAGE datasets are acquired as part of the MRI protocol. Alternatively, if the protocol comprises qMRI techniques for generating T1 and proton density (PD) maps, synthetic MP-RAGE datasets can be directly derived [9]. The advantage is that synthetic images are intrinsically corrected for inhomogeneities of the radio frequency (RF) field used for signal transmission (B1) and for non-uniformities of the receive coil profile (RP). Furthermore, they are in perfect anatomical alignment with the underlying qMRI datasets, allowing for improved accuracy of the qMRI analysis.

A method for the calculation of synthetic MP-RAGE datasets with either pure T1-weighting or T1-weighting combined with PD effects was published previously [9]. For segmentation purposes, the latter are more useful as they replicate more closely the contrasts in conventional MP-RAGE datasets.

The goal of this study was to further improve the method for obtaining synthetic T1-weighted MP-RAGE images with the specific aim to achieve more accurate tissue segmentation results. The following two improvements were introduced:

- Improved T1-mapping: the algorithm for T1 calculation was extended to correct for effects of B0 inhomogeneities on the water-selective excitation pulses.
- Improved derivation of MP-RAGE images: T1-based pseudo-PD maps, rather than actually measured PD maps, were used for the calculation.

2. Material and methods

2.1. Participants

Since the performance of tissue segmentation can be influenced by the presence of cerebral pathologies, the method was tested both on healthy control subjects and on patients. The patient group comprised patients with small or unremarkable pathologies (epilepsy patients) and patients with obvious diffuse and focal pathology (MS patients). In summary, 10 patients (1 male) with relapsing-remitting MS (RRMS), 10 patients (7 male) with focal epilepsy (9 patients with focal cortical dysplasias, 1 MRI negative patient) and 10 healthy control subjects (8 male) were recruited. The study was approved by the local ethics committee. Written informed consent was given by each participant. The investigation was conducted according to the principles expressed in the Declaration of Helsinki.

2.2. Data acquisition

Data were acquired on a 3 Tesla (T) whole body MR scanner with a body coil for RF transmission and an 8-channel phased-array head coil for RF reception (Trio, Siemens Medical Solutions, Erlangen, Germany). Data processing was performed with custom-made programs using FSL (FMRIB, Oxford) [10], FreeSurfer (Athinoula A. Martinos Center for Biomedical Imaging, Boston) [11] and MatLab (MathWorks, Natick, MA).

For mapping of T1 and PD, the VFA method was used with a FLASH-EPI hybrid readout [12] to improve the signal-to-noise ratio (SNR). The VFA method is based on the acquisition of at least two gradient echo datasets with different excitation angles and thus different degrees of T1-weighting, so T1 can be derived from the contrast differences. The acquisition parameters were: bandwidth (BW) = 222 Hz/Pixel, field-of-view (FOV): $256 \times 224 \times 160\,mm^3$ with a resolution of 1 mm isotropic, TR = 16.4 ms, TE = 6.7 ms, $\alpha_1 = 4^\circ$, $\alpha_2 = 24^\circ$, acquisition time: 9: 48 min. Fat-insensitive excitation pulses were used by subdividing each excitation pulse into two pulses with half the excitation angle, separated by a delay of 1.2 ms. While water spins remain in phase, so the combination of both pulses yields an effective excitation by the full angle, lipid spins at a field strength of 3 Tesla will experience a 180° phase drift during this delay, yielding a cancellation of the effects of both excitation pulses [13].

B1 was mapped as previously described in the literature [14] acquiring two GE datasets, one of which is preceded by an RF preparation pulse which causes a reduction of the longitudinal magnetization. Consequently, the quotient of both datasets yields the cosine of the actual preparation pulse angle, so B1 can be derived from comparison with the nominal value. The acquisition parameters were: BW = 260 Hz/Pixel, FOV: as above but with a resolution of 4 mm isotropic, TR = 11 ms, TE = 5 ms, $\alpha = 11^\circ$, acquisition time: 0:53 min.

To compensate for T2* related signal losses during the finite TE of the VFA datasets (which is required to obtain unbiased PD maps), two GE datasets with different TE were acquired: BW = 292 Hz/Pixel, FoV: as above with a resolution of 2 mm isotropic, TR = 16.7 ms, TE1 = 4.3 ms, TE2 = 11 ms, $\alpha = 50^\circ$, acquisition time: 5 min.

For B0 mapping, the methodology depended on the subjects investigated.

In the case of the patients with epilepsy, a standard B0 mapping method was included in the protocol, based on the acquisition of two GE datasets with different TE: BW = 200 Hz/Pixel, FoV: $256 \times 224 \times 160\,mm^3$ with a resolution of 4 mm isotropic, TR = 560 m, TE1 = 4.89 ms, TE2 = 7.35 ms, $\alpha = 60^\circ$, acquisition time: 1:03 min.

In the case of the MS patients and the healthy subjects, this sequence was omitted since the protocol comprised a T2* mapping method with export of modulus and phase data which allows for B0 mapping. The method was based on the acquisition of eight multiple-echo GE datasets: BW = 299 Hz/Pixel, FoV: $240 \times 180 \times 119\,mm^3$ with a resolution of $1.3 \times 1.3 \times 2mm^3$, TR = 60 m, TE1 = 10 ms, ΔTE = 6 ms, $\alpha = 30^\circ$, acquisition time: 5:46 min.

Table 1 summarizes the similarities and differences of the qMRI protocols used for the different subject groups.

Conventional MP-RAGE [15] datasets were measured as part of the study protocol for the epilepsy patients, only. The parameters were: BW = 170 Hz/Pixel, FoV: $256 \times 256 \times 192\,mm^3$ with a resolution of 1 mm isotropic, TR = 1900 ms, TE = 3.04 ms, TI = 900 ms, $\alpha = 9^\circ$, acquisition time: 4:28 min.

2.3. Data analysis

2.3.1. Standard method

B1 mapping: B1 maps were derived from the data as described above and in the literature [14]. T1 mapping: For compensation of subject movement effects, the PD-weighted dataset was coregistered to the T1-weighted dataset using FSL FLIRT. For T1 calculation, the standard VFA analysis was used. In summary, the method is based on the two datasets obtained with different effective excitation angles (α_1 and α_2) resulting in two different local signal amplitudes (S_1 and S_2). $S_i/\tan(\alpha_i)$ was plotted versus $S_i/\sin(\alpha_i)$, resulting in a linear graph with the slope $m = \exp(-TR/T1)$ from which T1 can be derived [16]. Before the calculation, all angles were corrected for B1 inhomogeneities. For correction of insufficient spoiling of transverse magnetization, a previously reported method was used [17], assuming that the VFA method yields an apparent T1 value T1(app) from which the correct T1 can be calculated according to $T1 = P1(B1) + P2(B1) * T1(app)$. The B1-dependent parameters P1(B1) and P2(B1) where chosen as suggested in

Table 1
Similarities and differences of the two qMRI protocols used for the different subject groups.

qMRI protocol	MS patients, healthy subjects	Epilepsy patients
Identical	- Acquisition of VFA data - B1 mapping - Compensation for T2* related signal losses	
Different	B0 maps derived from eight GE datasets with different TE, used for T2* mapping. Parameters: BW = 299 Hz/Pixel, FoV: 240 × 180 × 119 mm^3 Resolution: 1.3 × 1.3 × 2 mm^3, TR = 60 ms TE1 = 10 ms, ΔTE = 6 ms, α = 30° Acquisition time: 5:46 min. Conventional MP-RAGE: not included	B0 maps derived from two GE datasets with different TE. Parameters: BW = 200 Hz/Pixel FoV: 256 × 224 × 160 mm^3 Resolution: 4 mm isotropic, TR = 560 ms TE1 = 4.89 ms, ΔTE = 2.46 ms, α = 60° Acquisition time: 1:03 min. Conventional MP-RAGE: included
Total acquisition time	21:27 min	21:11 min

[18]:

$$P_1 = -31.6 \cdot B1^2 + 127 \cdot B1 - 59.5 \quad (1)$$

$$P_2 = 0.0552 \cdot B1^2 - 0.328 \cdot B1 + 1.17 \quad (2)$$

PD mapping: The PD-weighted dataset was first corrected for any B1, T1, and T2* bias. The resulting dataset therefore represents the product of the PD map and a bias with low spatial frequencies, imposed by non-uniformities of the specific profile of the receive coil (RP). The latter was removed from the data via bias field correction, using FSL FAST [19]. This software performs bias field correction as the first step of a tissue segmentation algorithm and can therefore be used for the sole purpose of correcting input data for bias fields. PD maps were scaled to a value of 100 percent units in CSF. The whole procedure has been described in detail in the literature [18].

Calculation of standard synthetic images: Synthetic MP-RAGE datasets with mixed PD and T1 weighting were calculated with the equations given in [9], assuming the following virtual acquisition parameters: TR = 1900 ms, TI = 900 ms, α = 9°, echo spacing 8.1 ms, 192 phase encoding steps inside the inner loop with symmetric k-space coverage. The parameters FoV, matrix size and spatial resolution were identical to the respective parameters of the underlying T1 and PD maps and thus of the VFA measurement.

2.3.2. Improved method

B1 mapping was identical to the standard method. B0 mapping: B0 was derived from the respective GE phase data acquired at different TE, using FSL PRELUDE and FUGUE. T1 mapping: Local excitation angles were first corrected for B1 inhomogeneities, as described for the standard method. Subsequently, for each pixel the effect of B0 distortions on the water-selective excitation was determined. For this purpose, the combined action of the two excitation pulses and the intermediate B0 related phase drift during the delay of 1.2 ms was determined via concatenation of the respective rotation matrices, allowing the deduction of the effective local excitation angle from the resulting magnetization vector. Effective excitation angle maps were derived both for the PD and the T1 weighted measurement. To correct for insufficient spoiling of transverse magnetization, a method recently proposed in the literature [20] was used which converts the effective excitation angles (α) into apparent values (α′) for which the Ernst Equation is valid, allowing for the direct application of the VFA algorithm. More in detail, apparent angles are calculated according to $\alpha' = C^*\alpha$ where the correction factor C follows from:

$$C = \sum_{k,l=0}^{k+l\leq 5} P_{k,l} \cdot \alpha^k \cdot TR^l \quad (3)$$

where α is given in deg. and TR is given in ms. The parameters $P_{k,l}$ where chosen as listed in the literature [20]. Using the apparent angle maps, T1 maps were derived with the VFA method as described in detail above in Section 2.3.1. (first paragraph).

PD mapping: Pseudo PD maps were calculated from the B0 corrected T1 maps with the Fatouros equation $1/PD = k_1 + k_2/T1$ [21,22], assuming the values $k_1 = 0.858$, $k_2 = 522$ ms. At 3 Tesla, this choice yields pseudo PD values that closely match the true values [23]. It should be noted that these pseudo PD maps are intrinsically corrected for B0 inhomogeneities as they are derived from the B0 corrected T1 maps.

Calculation of improved synthetic images: The calculation was identical to the standard case described above, but using the B0 corrected T1 and pseudo PD maps.

2.3.3. Segmentation, visual inspection and group analysis

Whole brain segmentation of the standard and the improved MP-RAGE datasets was performed with the “recon-all” command implemented in the Freesurfer toolbox [11,24]. Segmentation results were compared by visual inspection with “freeview”. In case relevant parts of cerebral tissue were misclassified, segmentation was considered to be insufficient. In the case of only small inaccuracies affecting few gyri, which can be easily corrected manually, segmentation was rated to be sufficient.

To visualize the distribution of the artifacts in the standard synthetic MP-RAGE images, PD maps of the healthy subjects were transferred to the Freesurfer space and PD values were read between 40 and 60% of the cortical thickness. The resulting surface datasets were normalized (“fsaverage” space) and smoothed with a Gaussian kernel with a full width at half maximum of 15 mm to allow for general linear model (GLM) analysis for the comparison of the cortical PD values resulting from the segmentation of the standard and the improved MP-RAGE datasets.

For quantitative comparison of the standard and the improved T1 maps on group level, brain-extracted synthetic MP-RAGE datasets were normalized to MNI 152 space with FSL FNIRT after initialization with FSL FLIRT. The respective coregistration matrices were applied to the brain-extracted T1 maps for normalization. Average T1 maps across all subjects were calculated both for the standard and the improved T1 maps. The relative difference of these maps was obtained by dividing the difference between the improved and the standard averaged T1 maps by the mean of both maps for each voxel. For avoidance of edge artifacts, the relative difference map was eroded with a 3 × 3 × 3 mm kernel and smoothed with a Gaussian kernel (sigma = 2 mm).

For the further investigation, a reference T1 map was obtained in the following way: first, mean white matter (WM) and gray matter (GM) T1 values were derived by averaging T1 values across WM or GM masks, respectively, which were derived from FSL FAST. Subsequently, WM and GM partial volume estimate (PVE) maps were used as weighting factors and a reference T1 map was calculated for each pixel by averaging the mean T1 values of WM and GM using the local weighting factors, according to: REF = PVE(WM) ∗ Mean_T1(WM) + PVE(GM) ∗ Mean_T1(GM). Subsequently, both the standard and the improved T1 maps (averaged across subjects)

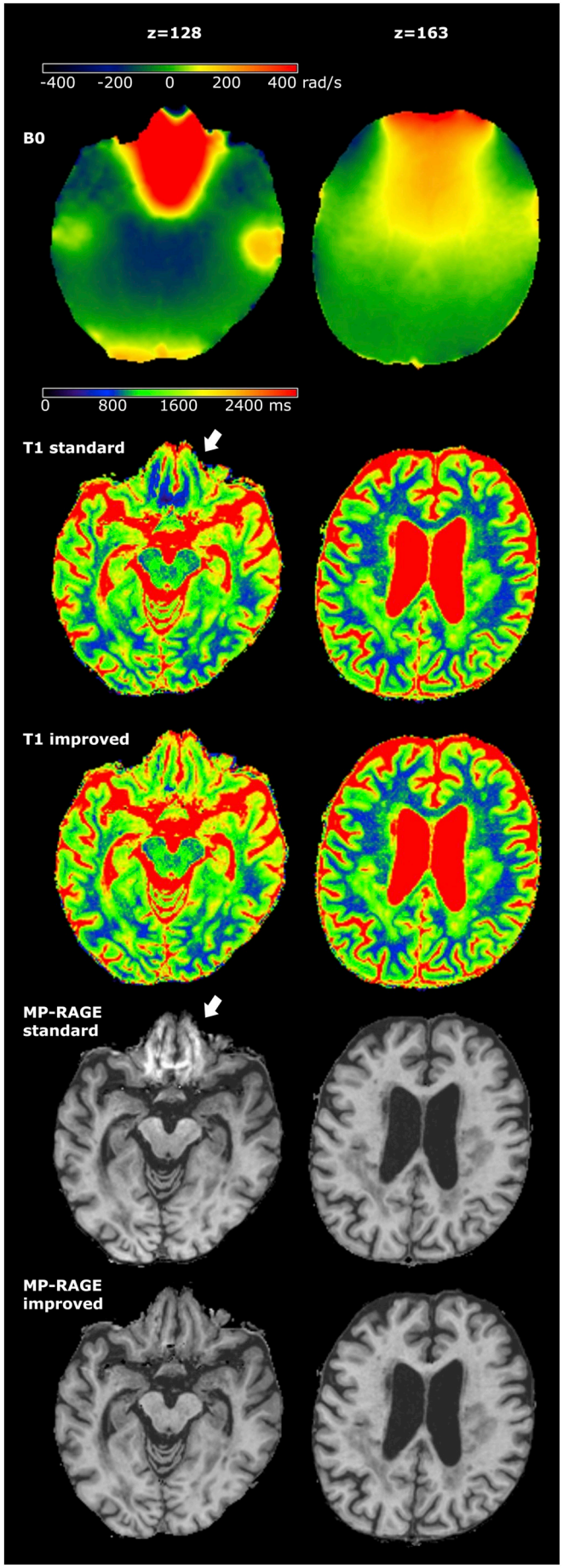

Fig. 1. The effect of B0 inhomogeneities on the standard and improved T1 maps and synthetic images. Relevant datasets for a basal (left) and a mid-cerebral slice (right), showing B0 maps (top), standard/improved T1 maps (middle) and standard/improved synthetic MP-RAGE images (bottom). Improved images show less artifacts in basal regions where pronounced B0 inhomogeneities are observed. Artifacts are marked with arrows.

were divided by this reference map. In theory, this quotient should be close to 1 (or 100%). Quotient maps were investigated for areas with marked deviations from this value.

In addition, ten conventional MP-RAGE datasets acquired for the patients with epilepsy were inspected for artifacts and compared visually with the synthetic images. For a more quantitative analysis, a comparison of histograms was performed between four datasets of the respective patients: the standard and improved synthetic images, the original uncorrected conventional MP-RAGE datasets and bias-field corrected versions of the conventional MP-RAGE data. The latter data were considered as the gold standard for assessing the quality of the synthetic anatomies. Bias correction was performed via the method N4 as described by Tustson et al. [25]. Histograms of signal intensities were obtained for voxels in a combined WM and GM mask. For easier comparison, data and histograms were scaled in a way that the median value in WM was 1000 and the histogram had a maximum peak amplitude of 1. For each of the four types of MP-RAGE datasets, the respective histograms were displayed both individually for all patients and averaged across patients. The standard deviations were presented with the same scaling.

Furthermore, it was aimed to provide a quantitative measure for the segmentation accuracy in basal regions and to compare this accuracy between the gold standard (N4-corrected conventional MP-RAGE images [25]) and the standard/improved synthetic datasets. For this purpose, cortical PD values were collected in the middle 20% of the cortical layer in the basal cortical regions, where segmentation errors due to B0 effects are most likely to occur and which were identified as described in the 2nd paragraph of Section 2.3.3. The rationale behind this procedure is that segmentation inaccuracies can be expected to yield decreased PD values due to partial volume effects with WM. This analysis was performed for each subject and each type of MP-RAGE dataset. PD values were compared via paired *t*-tests. It should be noted that conventional MP-RAGE images were only available for the patients with epilepsy.

3. Results

Mean values and standard deviations of the age of the patients and healthy subjects were: RRMS patients 35.7 ± 10.34 years, epilepsy patients: 34.5 ± 11.78 years, healthy subjects: 35.4 ± 12.55 years.

For demonstration, Fig. 1 shows two slices (columns) taken from datasets of an MS patient. The datasets comprise (rows): B0 map, standard and B0 corrected T1 map, standard and improved synthetic MP-RAGE. In the mid-cerebral areas (right column), B0 distortions are low, so T1 maps and synthetic T1-weighted images based on the standard and the improved method are virtually identical. In contrast, in basal frontal areas (left column) there are marked B0 inhomogeneities, so improved T1 maps and improved synthetic MP-RAGE datasets show less artifacts than the respective results based on the standard method (areas marked with white arrow).

Segmentation of the standard synthetic MP-RAGE datasets was rated insufficient in 6 out of 10 patients with epilepsy, 7 out of 10 patients with RRMS and 7 out of 10 healthy control subjects. The improved datasets allowed for satisfactory segmentation results in all but two cases: for one epilepsy and one RRMS patient segmentation was inadequate. Segmentation failures for standard synthetic MP-RAGE datasets were most pronounced in the MS group.

The results of the tissue segmentation for the different subject

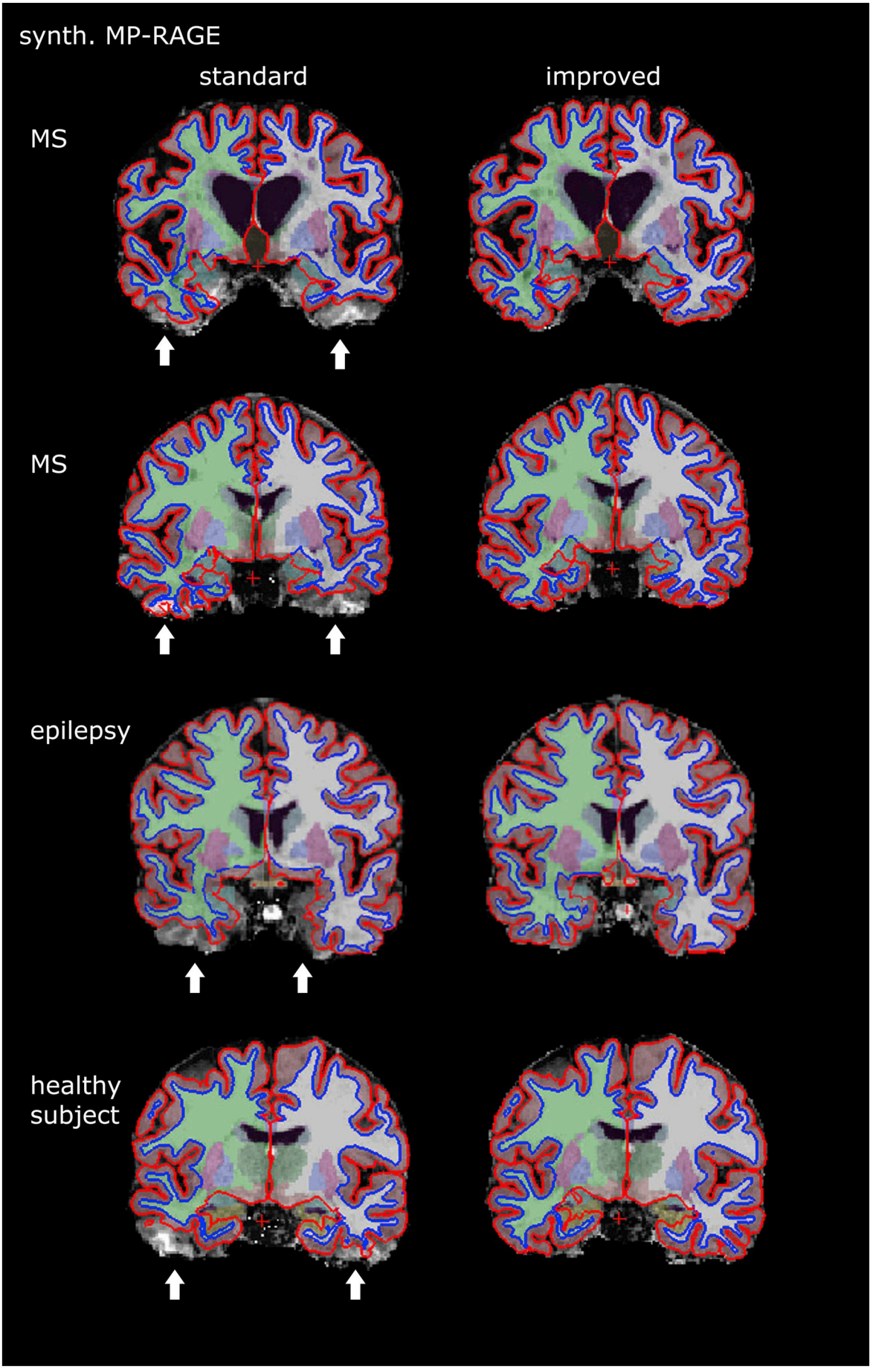

(caption on next page)

Fig. 2. Representative MP-RAGE images of patients with RRMS, epilepsy and healthy subjects in coronal view. The standard images are shown on the left side and the improved MP-RAGE datasets on the right side. The lines indicate segmentation results, representing the WM-GM boundary (blue) and the pial surface (red). Artifacts are marked with arrows. (For interpretation of the references to colour in this figure legend, the reader is referred to the web version of this article.)

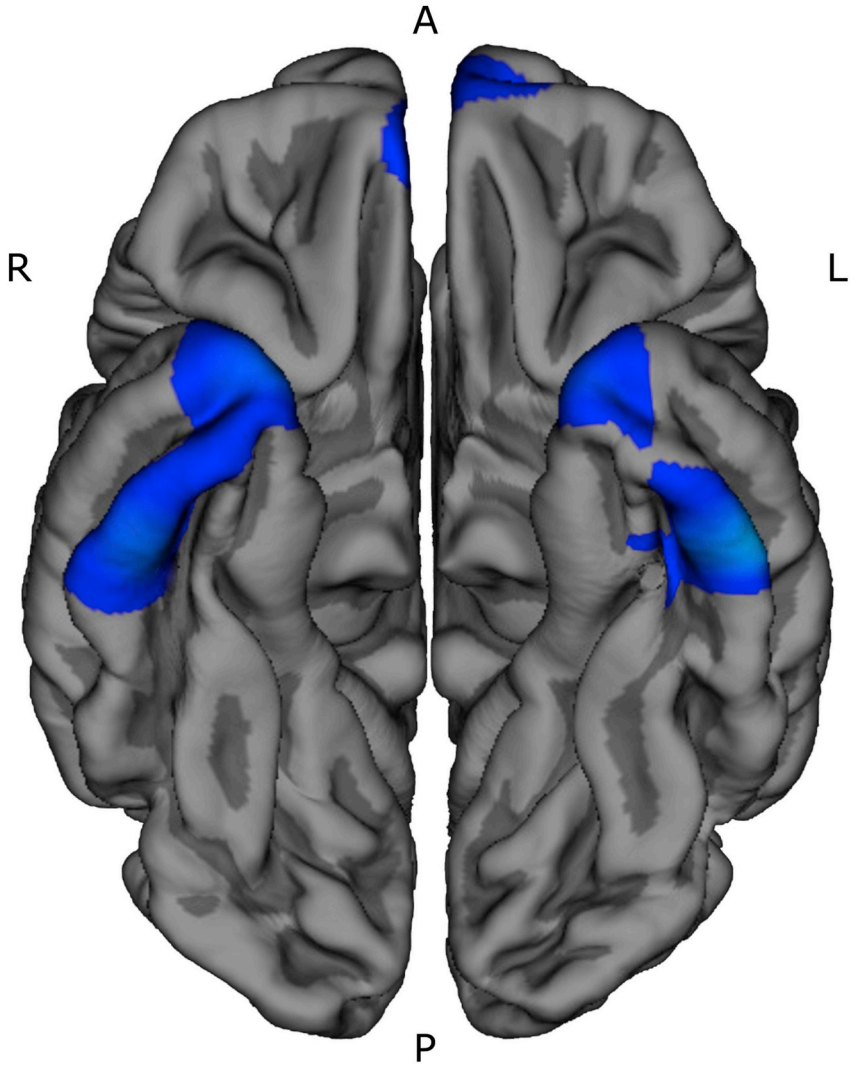

Fig. 3. Clusters with decreased cortical PD values in case the segmentation was performed on basis of the standard MP-RAGE datasets. Differences between segmentation results based on standard and improved data are only observed in basal regions.

groups are shown in Fig. 2, comparing standard (left) and improved (right) datasets. The crucial results of the respective segmentations are shown as a blue line, indicating the border between WM and cortical GM, and a red line, indicating the pial surface. The improved synthetic images show less artifacts and better segmentation results in basal frontal and temporal regions (areas marked with white arrows).

In case the segmentation was performed on the standard MP-RAGE datasets, rather than the improved datasets, clusters with decreased cortical PD values were observed in basal frontal and temporal regions (Fig. 3). These PD decreases were likely caused by partial volume effects with WM in regions with inaccurate segmentation of the standard MP-RAGE datasets, due to artifacts in these regions.

Analysis of the relative difference between T1 values obtained from the standard and the improved T1 maps (normalized average across all subjects) indicates discrepancies between the maps in some brain areas, in particular in the basal frontal and temporal regions and in the brainstem (Fig. 4). In these areas, T1 values were found to be lower in the standard T1 maps (Figs. 4; 5, top) which can be attributed to B0 distortions. In contrast, T1 values were similar in all other brain regions (Fig. 4). In particular, prominent T1 decreases in the standard T1 maps in the anterior, on the longitudinal axis middle pons and, accordingly, pontine artifacts in the standard MP-RAGE anatomies were observed in 18 out of 30 subjects. Suppl. Fig. 1 shows a respective artifact for a representative subject.

Division of the standard or improved T1 maps (averaged across all subjects) by a reference T1 map (based on averaged WM and GM T1 values) showed a strong deviation from the ideal value of 100% in basal frontal and brainstem regions for the standard T1 maps (demonstrated at group level in Fig. 5, bottom left). In contrast, this effect is strongly reduced in the B0 corrected maps (Fig. 5, bottom right).

Inspection of 10 conventional MP-RAGE datasets acquired for the patients with epilepsy did not unveil any of the above-mentioned basal artifacts. Synthetic datasets and uncorrected/bias-field-corrected conventional images are shown for a representative subject in Suppl. Fig. 2. It should be noted that an RF coil bias is visible in the uncorrected conventional MP-RAGE datasets (red arrows), but not in the synthetic or the N4-corrected conventional images. Figs. 6 and 7 show the results of the quantitative comparison of conventional and synthetic MP-RAGE

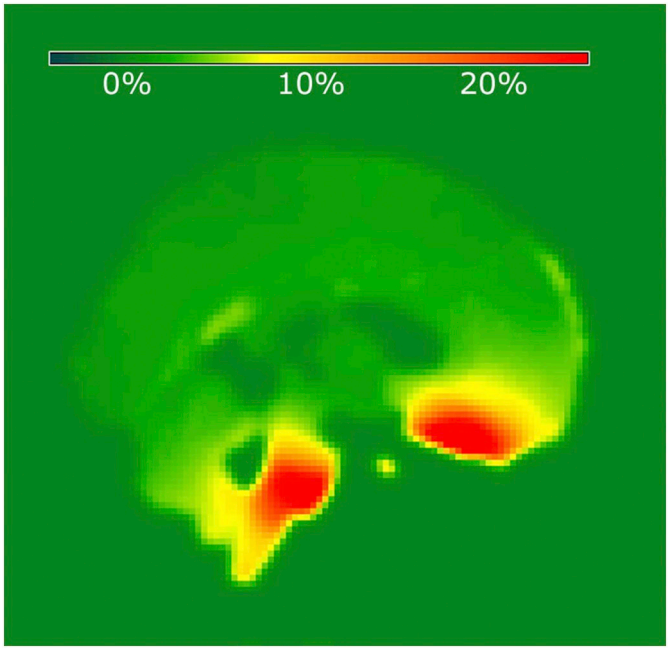

Fig. 4. The relative difference between standard and improved T1 maps, averaged across all subjects (sagittal slice, x = 46).

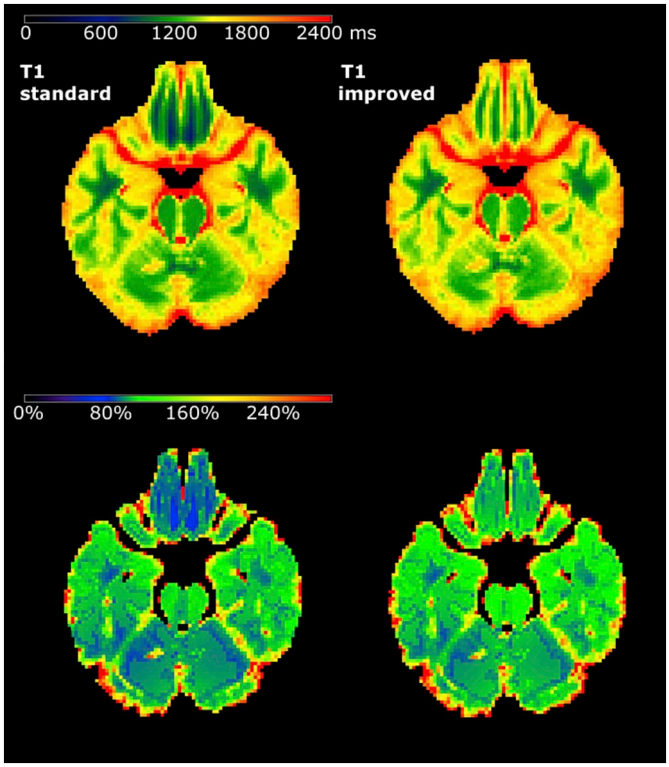

Fig. 5. Standard (left) and improved (right) T1 maps averaged across all subjects, showing the respective original maps (top) and the quotient of the original maps and a reference T1 map based on mean WM and GM T1 values (bottom) (z = 26).

datasets. Individual histograms (all patients, different colours) are shown in Fig. 6 for the uncorrected conventional (top left), bias-field-corrected conventional (gold standard, top, right), standard synthetic (bottom left) and improved synthetic (bottom right) MP-RAGE data. Furthermore, histograms averaged across all patients (left) and the respective standard deviations (right) are also shown for the different datasets in Fig. 7 (blue: standard synthetic MP-RAGE data, green: improved synthetic MP-RAGE data, red: uncorrected conventional MP-RAGE data, magenta: bias-field corrected conventional images). For the uncorrected conventional MP-RAGE data, the WM and GM peaks are not clearly separated, due to signal non-uniformities imposed by RF coil inhomogeneities. For the bias-corrected conventional and the synthetic MP-RAGE data, distinct peaks are visible. The dip between the peaks is more pronounced for the improved synthetic data and the corrected conventional datasets, indicating that the improved synthetic data are similarly well suited for discrimination between WM and GM as the gold standard data.

For estimation of the accuracy of the tissue segmentation, basal PD values were compared between the Freesurfer processed synthetic images and N4-corrected [25] conventional MP-RAGE datasets (gold standard), assuming that these values are decreased in the case of focal segmentation failures, due to resulting partial volume effects with WM. It should be noted that conventional MP-RAGE images were only available for the patients with epilepsy and that the conventional dataset needed to be excluded for one subject because the segmentation failed. PD values were lower for the standard synthetic images than for the gold standard in all 9 cases (standard synthetic: 75.0 ± 1.76, gold standard: 78.5 ± 1.83, $p < 0.01$) while results for the improved synthetic anatomies did not differ from the gold standard ($p = 0.41$) indicating appropriate segmentation. PD values were higher in 29 of 30 cases for the improved synthetic images than for the standard datasets ($p < 0.01$).

4. Discussion

In this study, two methods for the calculation of synthetic T1-weighted MP-RAGE images were compared. Synthetic datasets of this kind can be used for tissue segmentation and structural cerebral analysis of patients with neurological diseases such as epilepsy or MS. The standard synthetic datasets were constructed from T1 and PD maps according to a method published previously [9]. However, if standard methods are used for T1 and PD mapping, the resulting synthetic MP-RAGE images may suffer from artifacts in basal frontal and temporal regions (Figs. 1–3) which can hamper tissue segmentation (Fig. 2). The artifacts originated from two major causes. Firstly, the water-selective excitation pulses which are in general recommended for the acquisition of T1-weighted datasets to reduce ringing artifacts in the presence of subject movement [13] are strongly affected by basal B0 inhomogeneities, due to their frequency selective properties. Secondly, any artifacts in the originally acquired PD weighted dataset directly translate into the PD map and, accordingly, into the resulting standard synthetic MP-RAGE dataset.

For the calculation of the improved T1-weighted MP-RAGE images, a correction for B0 distortions was integrated in the underlying improved T1 mapping method, determining the effective excitation angles of the frequency selective pulses in the presence of B0 distortions. The PD information for the calculation of the improved images was obtained by converting T1 maps into pseudo PD maps, utilizing the Fatouros equation [23]. Importantly, the pseudo PD maps were based on B0 corrected T1 maps, so the resulting synthetic MP-RAGE datasets were likewise free from B0 inhomogeneities. Analysis revealed the higher quality of the improved T1 maps as demonstrated in Fig. 5, while the standard T1 maps showed a high deviation from mean WM and GM T1 values in basal regions.

Results showed that artifacts in basal regions were considerably reduced in the improved synthetic images. As a consequence, in contrast to the standard images, correct data segmentation was possible in the majority of cases. As shown in Fig. 3, PD values in the respective basal cortical regions appeared reduced when segmentation was based on the standard synthetic MP-RAGE datasets. These PD reductions were likely caused by partial volume effects with WM, thus allowing to visualize artifact patterns on the group level. This finding demonstrates

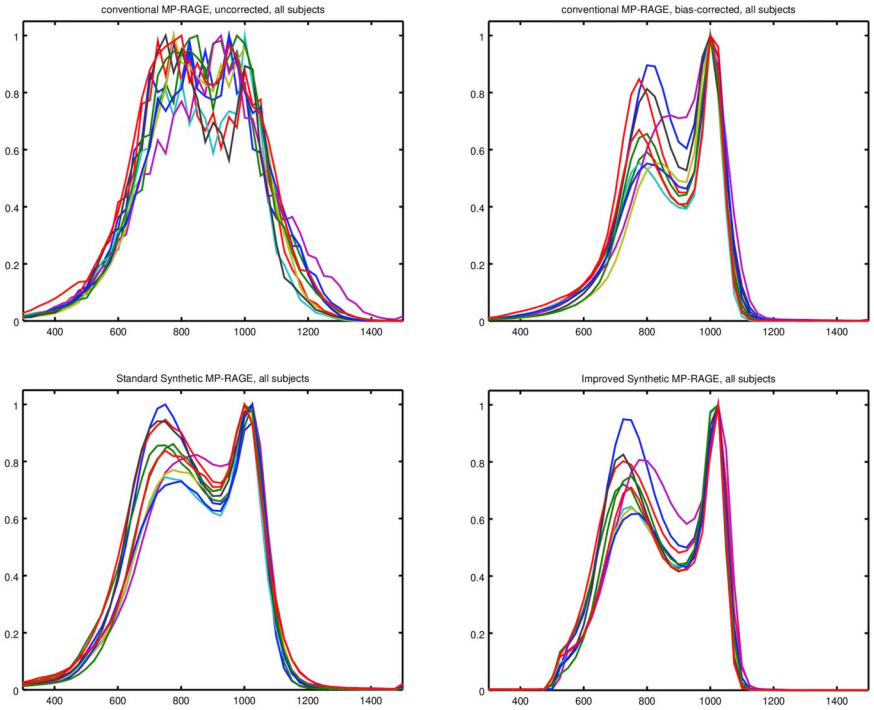

Fig. 6. Histograms for uncorrected (left, top) and bias-field-corrected (right, top) conventional MP-RAGE datasets and standard (left, bottom) and improved (right, bottom) synthetic images for the patients with epilepsy.

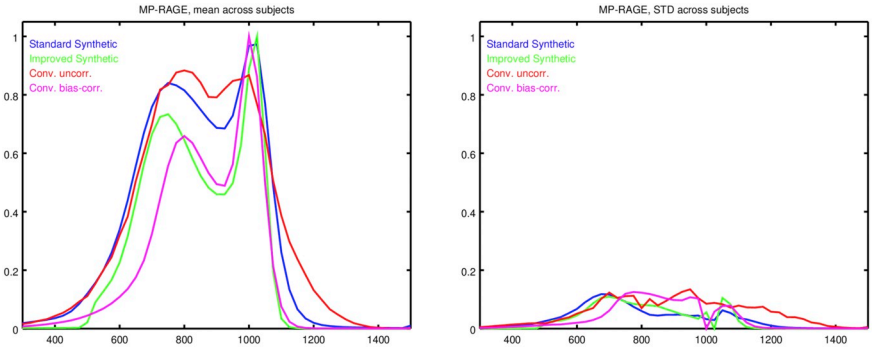

Fig. 7. Averaged histograms for the uncorrected/bias-corrected conventional and the standard/improved synthetic MP-RAGE datasets (left) and the respective standard deviations (SD, right).

the consequences of artifact related inaccuracies in synthetic images on cortical qMRI analyses and emphasizes the need for manual corrections in such cases.

The improved synthetic images allowed for a good WM/GM discrimination and appropriate segmentation results which were not inferior to results obtained for the gold standard data (N4-bias-corrected conventional datasets [25]). Bias-field correction is not required for the improved synthetic datasets which are intrinsically corrected for hardware effects.

B0 mapping has been used to correct for B0 dependent distortions in B1 maps in previous studies [26,27]. In this context, it has been highlighted that corrections of this kind are required at higher field strengths such as 7 T [27], due to the increased B0 inhomogeneities. The study presented here shows that even at a lower field strength of 3 T, B0 corrections should be performed when mapping T1 via the VFA method in combination with water-selective excitation pulses.

In clinical routine, conventional MP-RAGE datasets are standard. Still, it should be noted that the construction of synthetic MP-RAGE images provides advantages. For example, synthetic datasets have been shown to be beneficial for the visualization of brain tumors [9]. Furthermore, synthetic anatomical datasets derived via the MP2RAGE sequence provided a higher sensitivity regarding the assessment of the lesion load in MS patients than conventional MP-RAGE datasets [28]. Because the synthetic MP-RAGE datasets are directly derived from the T1 (and PD) maps, they are already given in the same geometrical space as the underlying quantitative maps. Thus, further coregistration is not required. This is of advantage, because each coregistration process is a potential source of error, which might in some cases affect the final results. Despite potential advantages, synthetic images can show artifacts. The present work describes a method for the improved calculation of synthetic images with reduced artifacts as compared to a previous method. In particular, the results suggest that for a study protocol comprising the acquisition of quantitative T1 maps, improved synthetic MP-RAGE images may replace conventional MP-RAGE datasets for the purpose of tissue segmentation, yielding reduced scan time. However, further research will be required to assess the value of synthetic datasets for different clinical questions and the comparability of qMRI data across scanner platforms. It has been demonstrated previously that qMRI based data may have a reduced inter-site bias for T1, PD and magnetization transfer saturation (MT) values [29]. Furthermore, it

was shown that GM probability maps based on MT values have a higher inter-site reproducibility as compared to the respective maps derived from T1-weighted data.

Interestingly, segmentation failures were most pronounced for standard synthetic images acquired on the RRMS group. A possible reason is that in this group, the occurrence of cerebral pathologies such as atrophy and MS lesions in itself can hamper the accurate detection of WM and GM borders and that additional artifacts enhance this effect. Segmentation failures in the standard datasets were found in basal regions only, where the majority of artifacts occurred for all subgroups. It should be noted that tissue or lesion segmentation in MS should also integrate T2-weighted images for better detection of lesions.

In summary, an improved method for the calculation of synthetic T1-weighted images was presented, which utilizes improved B0-corrected T1 maps and T1-based pseudo PD maps. The method reduces basal artifacts and allows for improved tissue segmentation. This technique allows all researchers who acquire quantitative T1 data to profit from the advantages of synthetic MP-RAGE datasets in neuroimaging studies.

Supplementary data to this article can be found online at https://doi.org/10.1016/j.mri.2019.05.013.

Declaration of Competing Interest

The authors report no conflicts of interest relevant to this study.

Dr. R Deichmann received compensation as a Consultant for MR scanner procurement by the Wellcome Trust Centre for Neuroimaging, UCL, London, UK.

Dr. F Rosenow has received honoraria for presentations and consultations from EISAI, UCB Pharma, Desitin Arzneimittel, Hexal, Novartis, Medtronic, GW-Pharma, Shire, Sandoz and Cerbomed as well as research grants from UCB, European Union, Deutsche Forschungsgemeinschaft, European Science Foundation and the Hessonian Ministries of Science and Arts and of Social Affairs and Integration.

Dr. S Knake has received speaker's honoraria from Desitin and UCB and educational grants from AD-Tech, Bial, Brainlab, Desitin, Eisai, Epilog, GW, Siemens, Philipps and UCB.

Dr. H Steinmetz has received speaker's honoraria from Bayer, Sanofi and Boehringer Ingelheim.

Acknowledgements

This work was supported by the State of Hesse with a LOEWE-Grant to the CePTER-Consortium (http://www.uni-frankfurt.de/67689811) and by the Clinician Scientists program at Goethe University. The sponsors did not influence the study design or the collection, analysis or interpretation of data.

References

[1] Cercignani M, Dowell NG, Tofts P, editors. Quantitative MRI of the brain: Principles of physical measurement. Boca Raton FL: CRC Press Taylor & Francis Group; 2018.
[2] Deichmann R, Gracien R-M. T1: Longitudinal relaxation time. In: Cercignani M, Dowell NG, Tofts P, editors. Quantitative MRI of the brain. Principles of physical measurement. Boca Raton FL: CRC Press Taylor & Francis Group; 2018.
[3] Gracien RM, Jurcoane A, Wagner M, Reitz SC, Mayer C, Volz S, et al. Multimodal quantitative MRI assessment of cortical damage in relapsing-remitting multiple sclerosis. Journal of Magnetic Resonance Imaging 2016;44:1600–7. https://doi.org/10.1002/jmri.25297.
[4] Gracien R-M, Jurcoane A, Wagner M, Reitz SC, Mayer C, Volz S, et al. The relationship between gray matter quantitative MRI and disability in secondary progressive multiple sclerosis. PloS one 2016;11:e0161036https://doi.org/10.1371/journal.pone.0161036.
[5] Vrenken H, Geurts Jeroen JG, Knol DL, Dijk van, Noor L, Dattola V, et al. Whole-brain T1 mapping in multiple sclerosis: global changes of normal-appearing gray and white matter. Radiology 2006;240:811–20. https://doi.org/10.1148/radiol.2403050569.
[6] Capraz IY, Kurt G, Akdemir Ö, Hirfanoglu T, Oner Y, Sengezer T, et al. Surgical outcome in patients with MRI-negative, PET-positive temporal lobe epilepsy. Seizure 2015;29:63–8. https://doi.org/10.1016/j.seizure.2015.03.015.
[7] Conlon P, Trimble MR, Rogers D, Callicott C. Magnetic resonance imaging in epilepsy: a controlled study. Epilepsy Res 1988;2:37–43. https://doi.org/10.1016/0920-1211(88)90008-3.
[8] Cantor-Rivera D, Khan AR, Goubran M, Mirsattari SM, Peters TM. Detection of temporal lobe epilepsy using support vector machines in multi-parametric quantitative MR imaging. Computerized Medical Imaging and Graphics 2015;41:14–28. https://doi.org/10.1016/j.compmedimag.2014.07.002.
[9] Nöth U, Hattingen E, Bähr O, Tichy J, Deichmann R. Improved visibility of brain tumors in synthetic MP-RAGE anatomies with pure T1 weighting. NMR Biomed 2015;28:818–30. https://doi.org/10.1002/nbm.3324.
[10] Smith SM, Jenkinson M, Woolrich MW, Beckmann CF, Behrens Timothy EJ, Johansen-Berg H, et al. Advances in functional and structural MR image analysis and implementation as FSL. NeuroImage 2004;23(Suppl. 1):19. https://doi.org/10.1016/j.neuroimage.2004.07.051.
[11] Fischl B, Sereno MI, Dale AM. Cortical surface-based analysis. II: inflation, flattening, and a surface-based coordinate system. NeuroImage 1999;9:195–207. https://doi.org/10.1006/nimg.1998.0396.
[12] Preibisch C, Deichmann R. T1 mapping using spoiled FLASH-EPI hybrid sequences and varying flip angles. Magn Reson Med 2009;62:240–6. https://doi.org/10.1002/mrm.21969.
[13] Howarth C, Hutton C, Deichmann R. Improvement of the image quality of T1-weighted anatomical brain scans. NeuroImage 2006;29:930–7. https://doi.org/10.1016/j.neuroimage.2005.08.004.
[14] Volz S, Nöth U, Rotarska-Jagiela A, Deichmann R. A fast B1-mapping method for the correction and normalization of magnetization transfer ratio maps at 3 T. NeuroImage 2010;49:3015–26. https://doi.org/10.1016/j.neuroimage.2009.11.054.
[15] Mugler JP, Brookeman JR. Three-dimensional magnetization-prepared rapid gradient-echo imaging (3D MP RAGE). Magnetic Resonance in Medicine 1990;15:152–7.
[16] Venkatesan R, Lin W, Haacke EM. Accurate determination of spin-density andT1 in the presence of RF-field inhomogeneities and flip-angle miscalibration. Magn Reson Med 1998;40:592–602. https://doi.org/10.1002/mrm.1910400412.
[17] Preibisch C, Deichmann R. Influence of RF spoiling on the stability and accuracy of T1 mapping based on spoiled FLASH with varying flip angles. Magn Reson Med 2009;61:125–35. https://doi.org/10.1002/mrm.21776.
[18] Volz S, Nöth U, Deichmann R. Correction of systematic errors in quantitative proton density mapping. Magn Reson Med 2012;68:74–85. https://doi.org/10.1002/mrm.23206.
[19] Zhang Y, Brady M, Smith S. Segmentation of brain MR images through a hidden Markov random field model and the expectation-maximization algorithm. IEEE Trans Med Imaging 2001;20:45–57. https://doi.org/10.1109/42.906424.
[20] Baudrexel S, Nöth U, Schüre J-R, Deichmann R. T1 mapping with the variable flip angle technique: a simple correction for insufficient spoiling of transverse magnetization. Magn Reson Med 2018;79:3082–92. https://doi.org/10.1002/mrm.26979.
[21] Fatouros PP, Marmarou A, Kraft KA, Inao S, Schwarz FP. In vivo brain water determination by T1 measurements: effect of total water content, hydration fraction, and field strength. Magn Reson Med 1991;17:402–13.
[22] Fatouros PP, Marmarou A. Use of magnetic resonance imaging for in vivo measurements of water content in human brain: method and normal values. J Neurosurg 1999;90:109–15. https://doi.org/10.3171/jns.1999.90.1.0109.
[23] Volz S, Nöth U, Jurcoane A, Ziemann U, Hattingen E, Deichmann R. Quantitative proton density mapping: correcting the receiver sensitivity bias via pseudo proton densities. NeuroImage 2012;63:540–52. https://doi.org/10.1016/j.neuroimage.2012.06.076.
[24] Dale AM, Fischl B, Sereno MI. Cortical surface-based analysis. I. Segmentation and surface reconstruction. NeuroImage 1999;9:179–94. https://doi.org/10.1006/nimg.1998.0395.
[25] Tustison NJ, Avants BB, Cook PA, Zheng Y, Egan A, Yushkevich PA, et al. N4ITK: improved N3 bias correction. IEEE Trans Med Imaging 2010;29:1310–20. https://doi.org/10.1109/TMI.2010.2046908.
[26] Lutti A, Hutton C, Finsterbusch J, Helms G, Weiskopf N. Optimization and validation of methods for mapping of the radiofrequency transmit field at 3T. Magn Reson Med 2010;64:229–38. https://doi.org/10.1002/mrm.22421.
[27] Lutti A, Stadler J, Josephs O, Windischberger C, Speck O, Bernarding J, et al. Robust and fast whole brain mapping of the RF transmit field B1 at 7T. PLoS ONE 2012;7:e32379https://doi.org/10.1371/journal.pone.0032379.
[28] Kober T, Granziera C, Ribes D, Browaeys P, Schluep M, Meuli R, et al. MP2RAGE multiple sclerosis magnetic resonance imaging at 3 T. Invest Radiol 2012;47:346–52. https://doi.org/10.1097/RLI.0b013e31824600e9.
[29] Weiskopf N, Suckling J, Williams G, Correia MM, Inkster B, Tait R, et al. Quantitative multi-parameter mapping of R1, PD*, MT, and R2* at 3T: a multi-center validation. Front Neurosci 2013. https://doi.org/10.3389/fnins.2013.00095.